

Acceleration of ACRs at the Termination Shock: 2-D Simulations

József Kóta* and J.R Jokipii*

*University of Arizona, Tucson, AZ 85721-0092, USA

Abstract. When Voyagers' crossed the termination shock (TS) in 2004 and 2007 the spectrum of anomalous cosmic rays (ACRs) did not unfold to a smooth power law at the shock. ACR fluxes continued to increase into the heliosheath and ACR spectra unfolded gradually as Voyagers advanced deeper into the heliosheath. This finding can be interpreted in terms of field-topology, i.e the connection between the Parker spiral field and the blunt termination shock.

We consider a two-dimensional model with an offset circle representing the blunt termination shock. Field lines wound in a Parker spiral cross the TS multiple times. We present simulation results with changing the shock strength and injection rate along the shock. We find that the flux of few MeV ACRs turn out sensitive to the injection rate at the nose and quite insensitive to the injection rate at the flank and tail regions. We also perform a backward calculation tracing the history of few MeV ACRs. Our results indicate that most of these ACRs, including ACRs in the tail, were likely be injected at the nose of the TS.

Keywords: Termination Shock, Acceleration, Anomalous Cosmic Rays

I. INTRODUCTION

Voyagers' crossing of the termination shock (TS) in 2004 and 2007 brought several surprises. First, the highly anisotropic precursor events were seen from the unexpected sunward direction [1]. This was interpreted in terms of Voyager's spiral magnetic field line intersecting the TS multiple times [2],[3]. The TS is not spherical but blunt [4], hence the first intersection of Voyager's field line is in the nose direction. Indeed Voyager-2 saw precursor events from the opposite, anti-sunward direction [5], in accordance with a blunt and asymmetric termination shock [6].

Second, both Voyager-1 [7],[8] and Voyager-2 [9], [5] found that anomalous cosmic rays (ACRs) did not unfold to a smooth power law at the shock. ACR fluxes continued to increase into the heliosheath and ACR spectra seen by both Voyagers unfolded gradually. This seemingly surprising finding could have been, in retrospect, anticipated as a result of insufficient time for acceleration at the nose [2]. McComas and Schwadron [10] suggested that ACRs are accelerated at the flanks, where connection time is longer and also conditions for injection is more favourable. This expectation has been confirmed by numerical simulations and theoretical arguments [11],[12],[13], [14].

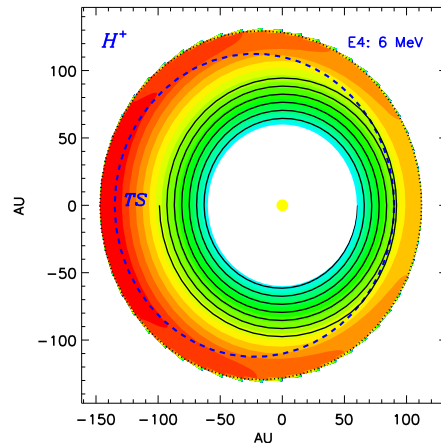


Fig. 1. Simulated 6 MeV ACR fluxes in a 2-D model heliosphere. The TS is an offset circle, intersected by the spiral field lines more than once. Red indicates high, blue indicates low intensity. ACR flux is depleted in the nose area and gradually increases farther out as diffusion fills up the frontal heliosheath.

Temporal variations in response to dynamical variations in the solar wind and the resulting motion of the TS were considered by Florinski and Zank [15]. The evolution of the ACR spectrum in the heliosheath is likely a combination of spatial and temporal changes. In this work we address spatial variations due to the blunt TS. We present numerical simulations in a 2-D model that captures the main topological feature of the blunt TS: spiral field lines intersect the shock several times.

II. SIMULATION RESULTS

We consider a 2-D model where the TS is represented by an offset circle, being at 90 AU and 135 AU heliocentric distances in the nose and tail direction, respectively. We solve Parker's diffusive transport equation [16], with anisotropic diffusion, taking $\kappa_{\perp} = 0.02\kappa_{\parallel}$. We assume no compression, hence no adiabatic heating or cooling, in the heliosheath. Our 2-D model represents a cone, latitudinal motion is not considered. Latitudinal displacement of ACRs due to particle drift along the TS is expected to become significant above ~ 10 MeV. Our simulation results are in broad qualitative agreement with Voyager observations [13].

Assuming a uniform injection rate along the shock, low-energy sub-MeV fluxes are more or less uniform everywhere along the shock since acceleration to low energies is fast and happens locally. At MeV energies, on the other hand, ACRs will be depleted at the nose

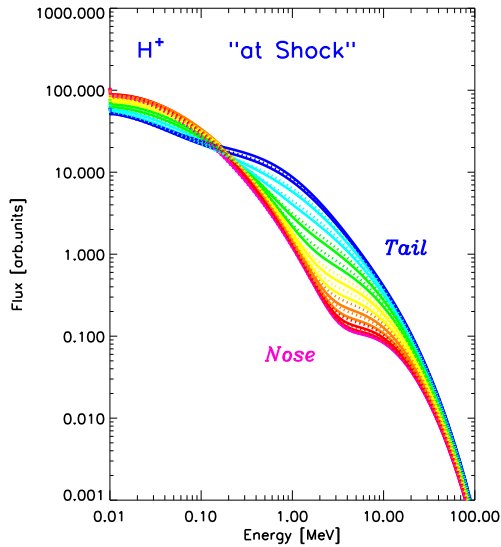


Fig. 2. Variation of the simulated spectrum along the shock face for the nose (red line) to the tail (blue). While spectra start uniformly at low energies they differ considerably at ACR energies.

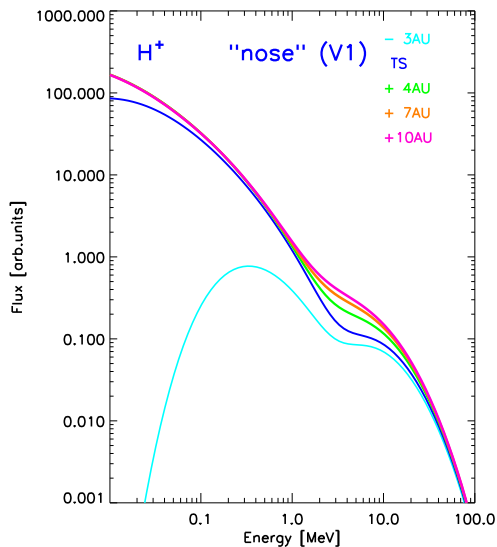


Fig. 3. Evolution of the simulated energy spectrum seen by Voyager-1 at different distances from the TS. The spectrum unfolds gradually.

due to the lack of sufficient time for acceleration to ACR energies. This is illustrated in Figures 1 and 2, showing our model simulation for the distribution of 6 MeV ACRs and the predicted variation of the spectrum along the TS.

The evolution of the energy spectrum predicted at different points of Voyager-1 trajectory is shown in Figure 3. The spectrum is heavily modulated inside the TS, appears still modulated at MeV energies at the shock, and unfolds gradually as the spacecraft moves farther out from the TS. This feature is further demonstrated in Figure 4, which depicts the simulated radial variation of particle fluxes along the trajectory of Voyager-1. Low-

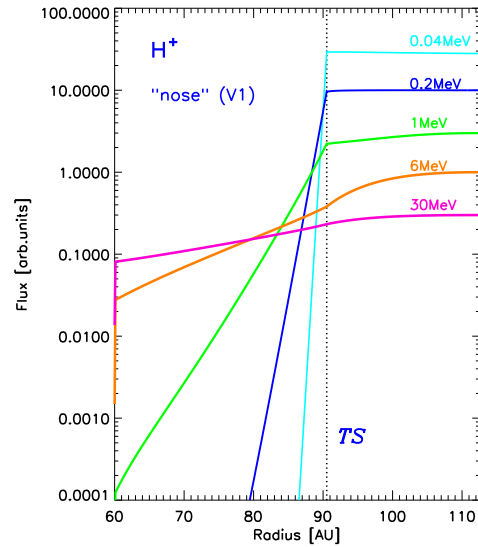


Fig. 4. Radial variation of the simulated particle fluxes along the trajectory of Voyager-1. While low energy fluxes are steady in the heliosheath, 6 MeV ACR fluxes continue to increase beyond the shock.

energy fluxes increase fast before the shock, and remain at a steady level beyond the TS in agreement with observations [8], [5]. MeV ACR fluxes, on the other hand, continue to increase after crossing the TS, in qualitative agreement with Voyager observations [7], [9].

III. BACKWARD TRACKING

We find that the qualitative features of our 2-D model simulation are quite robust and insensitive to the detailed profile of either the injection rate and or the shock strength along the shock. ACRs turn out depleted at and in the immediate front of the TS nose even if the shock is taken stronger at the nose and weaker towards the flanks and tail. The total flux is sensitive to the injection rate at the nose and insensitive to the injection rate chosen for the flanks and tail. All this suggest that most of the ACRs are injected and starts its life at the nose.

To trace back the likely history of ACRs from injection, through acceleration and transport, to become ACR at the nose, we performed a backward calculation. 5 MeV pseudo-particles are released from a location 5 AU off the nose of the TS, and their transport is followed by solving Parker's transport equation with the solar wind flowing sunward, and pseudo-particles being decelerated down to injection energy.

Simulation results are shown in Figure 5 and 6. What this calculation yields is the likelihood of a 10 keV particle injected at a given location to become a 5 MeV ACR and be detected at the nose of the TS. Inspection of Fig. 5 shows that particle injected at the nose have far better chance to be accelerated to high energies, since they get into acceleration process early. while particles injected at the tail are soon convected away and have less chance to return to the shock. The white color in heliosheath means that 10 keV particles starting in the

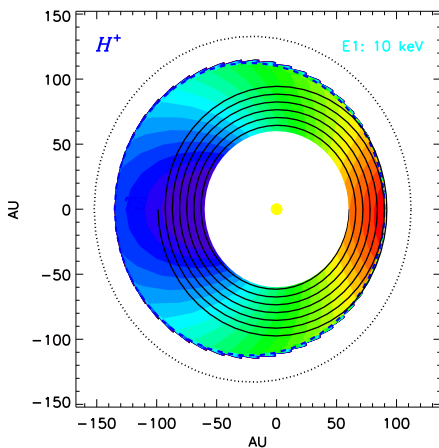


Fig. 5. Likelihood of a 10 keV in particle to become 5 MeV ACR to be detected at the nose of the TS. Injection at the nose gives higher likelihood (red). Particles injected in the heliosheath are convected away and have no chance (white).

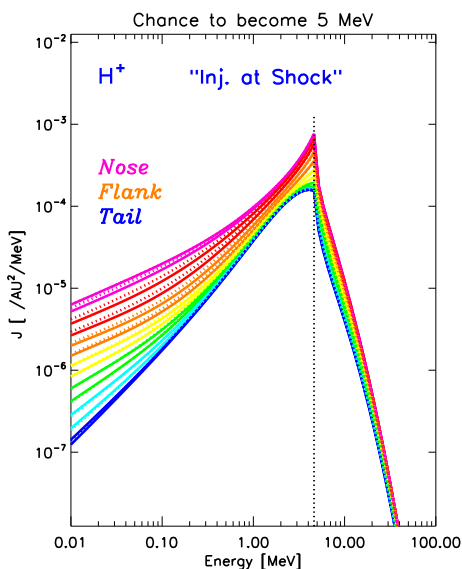


Fig. 6. Likelihood of a particle injected at various energies and at various places along the shock face to become a 5 MeV ACR and be detected at the nose of the TS. The high-energy branch above 5 MeV would imply deceleration inside the TS.

heliosheath have practically no chance to return to the shock and be accelerated.

The same qualitative conclusion is also demonstrated in Fig. 6, showing the chance of particles injected at various energies at various places along the shock to become 5 MeV ACR. The two branches of these curves imply that 5 MeV energy can be reached either from lower energy by acceleration at the TS, or from higher energy by adiabatic cooling inside the TS. Inspection of the low-energy branch shows that particles injected at the nose are more likely to be accelerated to ACR energies.

IV. SUMMARY

We presented simulation results that are in broad qualitative agreement with Voyager observations, supporting the interpretation of McComas and Schwadron [10]. This interpretation, of course, does not rule out that temporal variations may have also a role.

At the same time, we find that the qualitative features of our 2-D model predictions turn out quite robust for a broad range of parameters. The cross-field diffusion adopted in the present simulation is relatively small ($\kappa_{\perp}/\kappa_{\parallel} = 0.02$), but the qualitative features are present, with smaller magnitude, at $\kappa_{\perp}/\kappa_{\parallel} = 0.05$ as well. Qualitative results are also insensitive to the details of the longitudinal profile of injection rate and shock strength along the shock face.

Our simulations presented here strongly suggest that most of the MeV ACRs originate from seed particles injected at, or near to, the front of the TS. These particles are the ones that have the longest time for acceleration. During the acceleration process they then move toward the flanks as they tend to follow the motion of the field lines. While ACRs move toward the flanks during the acceleration process, their most likely 'birthplace' is the nose of the TS.

V. ACKNOWLEDGEMENTS

The authors benefited from discussions with E.C. Stone, R.B. Decker, and J. Giacalone. This work was supported by NASA under grants LWS04-0029-0003, NNX07AH19G, NNX08AQ14G, NNX09AB13G, and NNX09AG32G.

REFERENCES

- [1] S.M. Krimigis et al., *Nature*, **426**, 45 (2003)
- [2] J. Kóta and J.R. Jokipii, *AIPC* 719, 272 (2004).
- [3] J.R. Jokipii, J. Giacalone, and J. Kóta, *Astrophys. J.* **611**, L141 (2004).
- [4] G.P. Zank, *Space Sci. Rev.* **89**, 413 (1999).
- [5] R.B. Decker et al., *Nature*, **454**, 67 (2008)
- [6] M. Opher, E.C. Stone and T.I. Gombosi, *Science*, **316**, 8750 (2007).
- [7] E.C. Stone et al., *Science*, **309**, 2017 (2005).
- [8] R.B. Decker et al., *Science*, **309**, 2020 (2005).
- [9] E.C. Stone et al., *Nature*, **454**, 71 (2008)
- [10] D.J. McComas and N.A. Schwadron, *Geophys. Res. Lett.*, **33**, 4017 (2006).
- [11] J. Kóta and J.R. Jokipii, *AIPC* 858, 171 (2006).
- [12] N.A. Schwadron, M.A. Lee, and D.J. McComas, *Astrophys. J.* **675**, 1584 (2008).
- [13] J. Kóta and J.R. Jokipii, *AIPC* 1039, 397 (2008).
- [14] J.R. Jokipii and J. Kóta, *AIPC* 1039, 390 (2008).
- [15] V. Florinski and G.P. Zank, *Geophys. Res. Lett.* **33**, 110 (2006).
- [16] E.N. Parker, *Planet. Sp. Sci.* **13**, 9 (1965). *Astrophys. J.* **660**, 336 (2007).